IOSR Journal of Electronics and Communication Engineering (IOSR-JECE)
e-ISSN: 2278-2834, p- ISSN: 2278-8735.Volume 20, Issue 6, Ser. 2 (Nov – Dec 2025), PP 01-15
www.iosrjournals.org

Contribution Of Robust M-Analysis Of The Perturbed Longitudinal Flight System With Structured And Unstructured Uncertainties Of Missile

Shen Andriantsoa Ratsirarson, Andry Auguste Randriamitantsoa, Radoniaina Rasoamanana, Solofo Herizo Ranarison, Apotheken Gericha Rabearivelo

(Department Of Telecommunication, Doctoral School Of Engineering And Innovation Sciences And Techniques, University Of Antananarivo, Madagascar)
(Department Of Telecommunication, University Of Antananarivo, Madagascar)
(Department Of Electrical Engineering, University Of Antananarivo, Madagascar)

Abstract:
The concept of missile defence traces its root to the Cold War. In the present era, missiles development are constantly evolving and Air-to-air missiles are used on many modern military combat aircraft for self-defence. A control system for a missile is responsible for its attitude, while missile guidance system is responsible for controlling its trajectories. This paper aims at presenting the state of the art concerning the application of the robust mu-analysis techniques of linear systems of longitudinal flight of a missile. The introduced autopilot is implemented within the 6DOF simulation to check its robustness against non-modeled dynamics and nonlinearities. The non-linear 6DOF equations of motions are solved together to obtain the roll transfer function. The simulation results demonstrated the robustness capability in presence perturbed and noise.
Key Word: *Missile; state-space; robust control; μ-analysis; controller design*

Date of Submission: 13-12-2025 Date of Acceptance: 23-12-2025

I. Introduction

The missile guidance and control technologies are undergoing continuous advancement because the guidance and control system plays a key role in realizing the flight mission of missiles. The robust mu-analysis of a missile is a type of control of which the purpose is to guide the performance and stability of a system during flight face to uncertainties of the model and a difficult task since the dynamics of the system is no linear, unstable on certain flight ranges and has a strongly coupled dynamic. Indeed, the mathematical model that models a real system is a representation that aims to best approximate, with simplifying assumptions, the system we want to control.

II. Material And Methods

Analysis of the nominal system of a missile

The **Figure 1** represents the simulation diagram of the longitudinal flight of the missile.

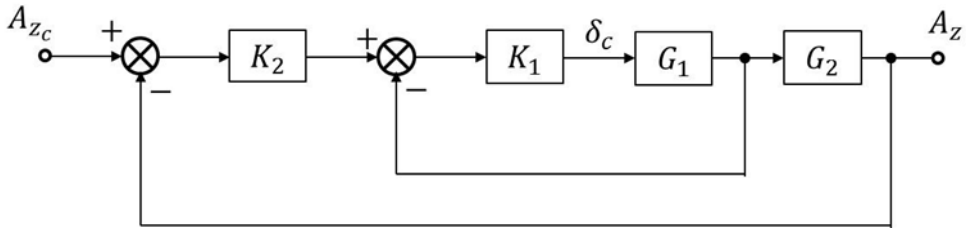

Figure 1: Control of the longitudinal flight of the missile.

The objective is to control the acceleration A_z by using the two possible measures:
- Acceleration A_{zc} ;
- Instantaneous rotational speed q.

δ_c is the servo command for the control surface. It is drawn up from the P.I. controllers which have respectively as transfer functions K_1 and K_2.

Longitudinal flight state-space equation

After linearization of the missile aerodynamic equations around a trim condition, we obtain the following equations:

$$\dot{\alpha}(t) = Z_a\alpha(t) + q(t) + Z_d\delta(t) \quad (1)$$
$$\ddot{\theta}(t) = \dot{q}(t) = M_a\alpha(t) + M_d\delta(t) \quad (2)$$
$$\dot{\delta}(t) = \delta(t) \quad (3)$$
$$\ddot{\delta}(t) = -\omega_n^2\delta(t) - 2\xi\omega_n\dot{\delta}(t) + \omega_n^2\delta_c(t) \quad (4)$$
$$q(t) = q(t) \quad (5)$$

The nominal values of the aerodynamic coefficients of the missile are:
- $Z_a = -1.3046$
- $M_a = 47.7109$
- $Z_d = -0.2142$
- $M_d = -104.8346$

The remaining parameters are:
- Missile velocity : $V = 886.78\ ft/s$
- Actuator damping ratio : $\xi = 0.6$
- Actuator natural frequency : $\omega_n = 113\ rad/s$

Longitudinal flight simulation

Figure 2 shows the block diagram of the system.

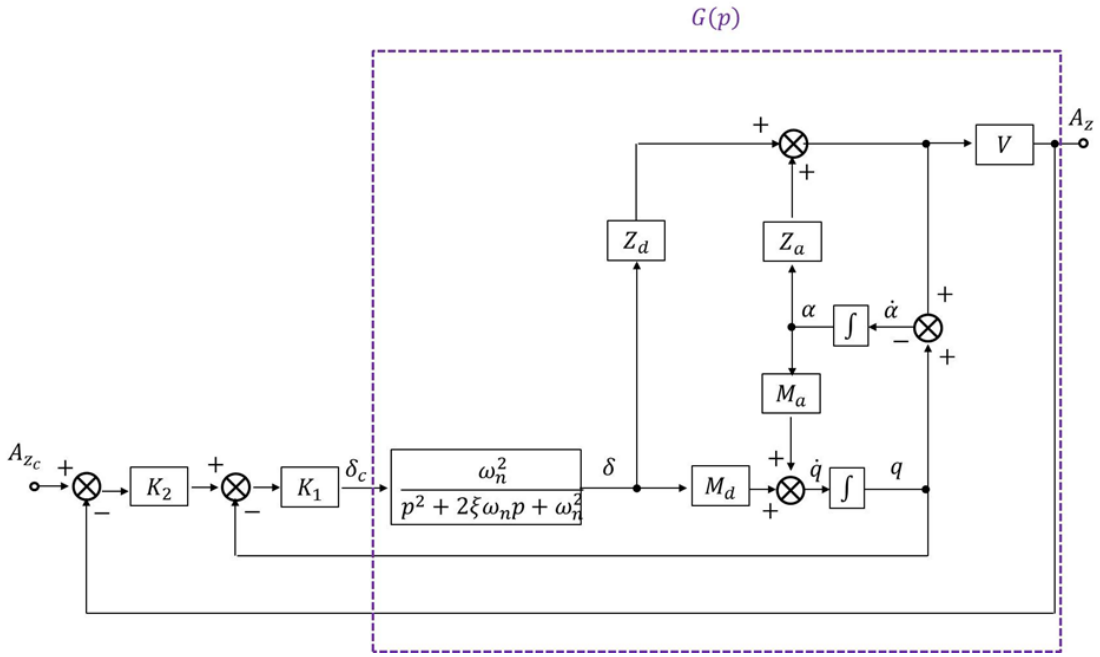

Figure 2: Block diagram of the longitudinal flight of the missile.

With :
- A_z : vertical acceleration command
- δ_c : fin deflection command
- δ : fin deflection angle
- q : instantaneous angular velocity

From (1), we have:

$$p\alpha(p) = Z_a\alpha(p) + q(p) + Z_d\delta(p) \quad (6)$$
$$(p - Z_a)\alpha(p) = q(p) + Z_d\delta(p) \quad (7)$$

Hence:

$$\alpha(p) = \frac{1}{p - Z_a} q(p) + \frac{Z_d}{p - Z_a} \delta(p) \tag{8}$$

From (2) we have:

$$pq(p) = M_a \alpha(p) + M_d \delta(p) \tag{9}$$

$$pq(p) = M_a \left[\frac{1}{p - Z_a} q(p) + \frac{Z_d}{p - Z_a} \delta(p) \right] + M_d \delta(p) \tag{10}$$

$$[p(p - Z_a) - M_a] q(p) = [Z_d M_a + M_d (p - Z_a)] \delta(p) \tag{11}$$

We obtain:

$$\frac{q(p)}{\delta(p)} = \frac{Z_d M_a + M_d (p - Z_a)}{p(p - Z_a) - M_a} \tag{12}$$

$$\frac{q(p)}{\delta(p)} = \frac{M_d p - M_d Z_a + Z_d M_a}{p^2 - Z_a p - M_a} \tag{13}$$

From (3) we have:

$$p^2 \delta(p) = -\omega_n^2 \delta(p) - 2\xi \omega_n p \delta(p) + \omega_n^2 \delta_c(p) \tag{14}$$

$$(p^2 + 2\xi \omega_n p + \omega_n^2) \delta(p) = \omega_n^2 \delta_c(p) \tag{15}$$

And we obtain:

$$\frac{\delta(p)}{\delta_c(p)} = \frac{\omega_n^2}{p^2 + 2\xi \omega_n p + \omega_n^2} \tag{16}$$

The transfer function $G_1(p)$ is written according to (13) and (16) :

$$G_1(p) = \frac{q(p)}{\delta_c(p)} \tag{17}$$

$$G_1(p) = \frac{\omega_n^2 [M_d p - M_d Z_a + Z_d M_a]}{(p^2 + 2\xi \omega_n p + \omega_n^2)(p^2 - Z_a p - M_a)}$$

From (4) we have

$$A_z(p) = V Z_a \alpha(p) + V Z_d \delta(p) \tag{18}$$

By replacing $\alpha(p)$ with the equation (18), we obtain:

$$A_z(p) = V Z_a \left[\frac{1}{p - Z_a} q(p) + \frac{Z_d}{p - Z_a} \delta(p) \right] + V Z_d \delta(p) \tag{19}$$

$$\frac{1}{V} A_z(p) = \frac{1}{p - Z_a} Z_a q(p) + \left(\frac{Z_d Z_a + Z_d (p - Z_a)}{p - Z_a} \right) \delta(p) \tag{20}$$

Yet:

$$\frac{q(p)}{\delta(p)} = \frac{M_d p - M_d Z_a + Z_d M_a}{p^2 - Z_a p - M_a} \tag{21}$$

$$\delta(p) = \frac{p^2 - Z_a p - M_a}{M_d p - M_d Z_a + Z_d M_a} q(p) \tag{22}$$

Hence:

$$\frac{1}{V} A_z(p) = \frac{1}{p - Z_a} Z_a q(p) + \left[\frac{Z_d Z_a + Z_d (p - Z_a)}{p - Z_a} \right] \left[\frac{p^2 - Z_a p - M_a}{M_d p - M_d Z_a + Z_d M_a} \right] q(p) \tag{23}$$

$$\frac{1}{V} A_z(p) = \left[\frac{1}{p - Z_a} Z_a + \frac{Z_d Z_a + Z_d (p - Z_a)}{p - Z_a} \cdot \frac{p^2 - Z_a p - M_a}{M_d p - M_d Z_a + Z_d M_a} \right] [q(p)] \tag{24}$$

$$\frac{1}{V} A_z(p) = \frac{(M_d p - M_d Z_a + Z_d M_a) Z_a + [Z_d Z_a + Z_d (p - Z_a)][p^2 - Z_a p - M_a]}{(p - Z_a)(M_d p - M_d Z_a + Z_d M_a)} q(p) \tag{25}$$

$$\frac{A_z(p)}{q(p)} = \frac{(M_d p - M_d Z_a + Z_d M_a) Z_a + [Z_d Z_a + Z_d (p - Z_a)][p^2 - Z_a p - M_a]}{(p - Z_a)(M_d p - M_d Z_a + Z_d M_a)} V \tag{26}$$

$$\frac{A_z(p)}{q(p)} = \frac{Z_a M_d p - M_d {Z_a}^2 + Z_a Z_d M_a + [Z_d Z_a + Z_d (p - Z_a)][p^2 - Z_a p - M_a]}{(p - Z_a)(M_d p - M_d Z_a + Z_d M_a)} V \tag{27}$$

Finally, we obtain:

$$G_2(p) = \frac{A_z(p)}{q(p)}$$

$$G_2(p) = \frac{V[Z_d p^2 - (Z_d M_a - Z_a M_d)]}{[M_d p + (Z_d M_a - Z_a M_d)]} \tag{28}$$

Robust control of the longitudinal flight

We propose to analyze the robustness of the longitudinal flight control system of a missile with respect to uncertainties in the aerodynamic parameters.

The **Figure 3** represents the perturbed system.

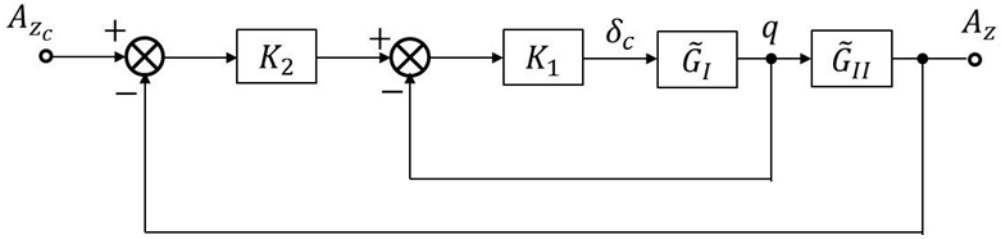

Figure 3: Block diagram of the perturbed system

The system parameters are subject to parametric uncertainty. Each uncertain coefficient $\tilde{p}_i \in \{\tilde{M}_a;\ \tilde{Z}_a; \tilde{M}_d; \tilde{Z}_d\}$ is represented as:

$$\tilde{p}_i = p_i(1 + \omega_i\delta_i), |\delta_i| < 1 \quad (29)$$

Where p_i ($p \in \{M_a;\ Z_a; M_d; Z_d\}$) is the nominal value of the considered parameter and ω_i ($\omega_i \in \{\omega_{M_a}; \omega_{Z_a}; \omega_{M_d}; \omega_{Z_d}\}$) the coefficient of the corresponding weighting. $\omega_i = 0{,}2$ is chosen for all parameters.

Using the upper linear fractional transformation, we have:

$$\tilde{p}_i = [Q_{22} + Q_{21}\Delta_u(I - Q_{11}\Delta_u)^{-1}Q_{12}] \quad (30)$$

Let :

$$Q_i = \begin{bmatrix} 0 & p_i \\ \omega_i & p_i \end{bmatrix} \quad (31)$$

Hence the block diagram of the perturbed system is shown in the **Figure 4**.

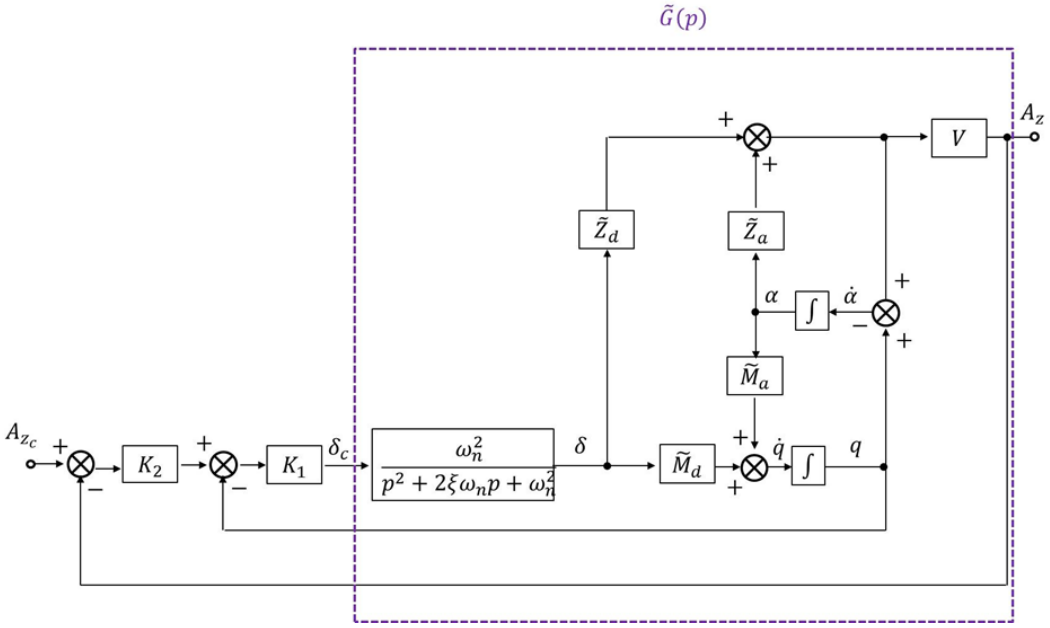

Figure 4: Block diagram of the perturbed system in longitudinal flight of the missile.

Simulation of $\tilde{M}_a$

Let use denote

$$\tilde{M}_a = M_a\left(1 + \omega_{M_a}\delta_{M_a}\right) \quad (32)$$

$$\tilde{M}_a = M_a + M_a\omega_{M_a}\delta_{M_a} \quad (33)$$

$$\tilde{M}_a = F_l\left[P_{M_a}, \delta_{M_a}\right] \quad (34)$$

$$\tilde{M}_a = P_{11} + P_{12}\delta_{M_a}\left[I - P_{22}\delta_{M_a}\right]^{-1}P_{21} \quad (35)$$

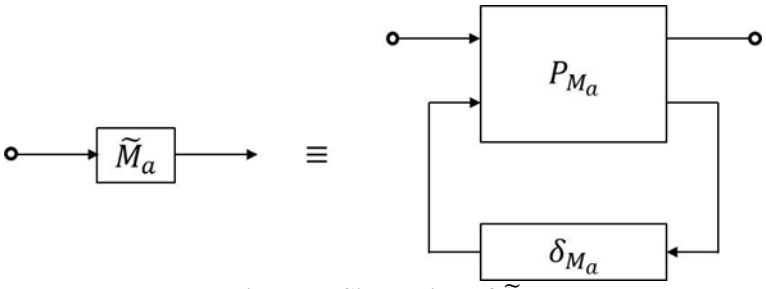

Figure 5: Simulation of $\widetilde{M}_a$

By identification, we obtain:

$$P_{M_a} = \begin{bmatrix} M_a & M_a\omega_{M_a} \\ 1 & 0 \end{bmatrix} \tag{36}$$

Simulation of $\widetilde{Z}_a$

Let use denote

$$\tilde{Z}_a = Z_a\left(1 + \omega_{Z_a}\delta_{Z_a}\right) \tag{37}$$

$$\tilde{Z}_a = Z_a + Z_a\omega_{Z_a}\delta_{Z_a} \tag{38}$$

$$\tilde{Z}_a = F_l\left[P_{Z_a}, \delta_{Z_a}\right] \tag{39}$$

$$\tilde{Z}_a = P_{11} + P_{12}\delta_{Z_a}\left[I - P_{22}\delta_{Z_a}\right]^{-1}P_{21} \tag{40}$$

By identification, we obtain:

$$P_{Z_a} = \begin{bmatrix} Z_a & Z_a\omega_{Z_a} \\ 1 & 0 \end{bmatrix} \tag{41}$$

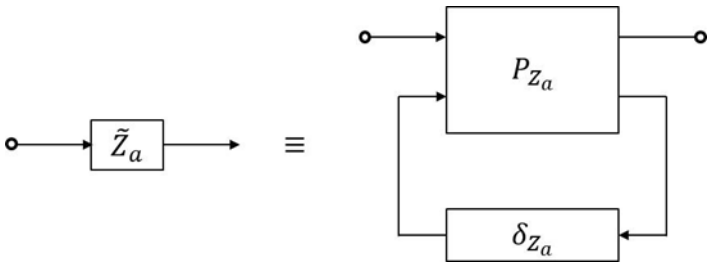

Figure 6: Simulation of $\widetilde{Z}_a$

Simulation of $\widetilde{M}_d$

Let use denote

$$\tilde{M}_d = M_d\left(1 + \omega_{M_d}\delta_{M_d}\right) \tag{42}$$

$$\tilde{M}_d = M_d + M_d\omega_{M_d}\delta_{M_d} \tag{43}$$

$$\tilde{M}_d = F_l\left[P_{M_d}, \delta_{M_d}\right] \tag{44}$$

$$\tilde{M}_d = P_{11} + P_{12}\delta_{M_d}\left[I - P_{22}\delta_{M_d}\right]^{-1}P_{21} \tag{45}$$

By identification, we obtain:

$$P_{Z_a} = \begin{bmatrix} M_d & M_d\omega_{M_d} \\ 1 & 0 \end{bmatrix} \tag{46}$$

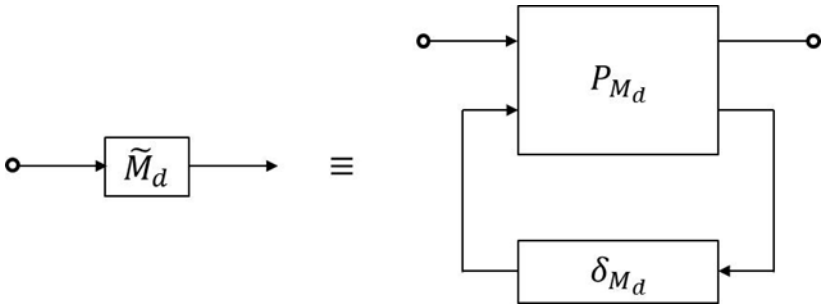

Figure 7: Simulation of $\widetilde{M}_d$

Simulation of $\tilde{Z}_d$

Let use denote

$$\tilde{Z}_d = Z_d\left(1 + \omega_{Z_d}\delta_{Z_d}\right) \quad (47)$$

$$\tilde{Z}_d = Z_d + Z_d\omega_{Z_d}\delta_{Z_d} \quad (48)$$

$$\tilde{Z}_d = F_l\left[P_{Z_d}, \delta_{Z_d}\right] \quad (49)$$

$$\tilde{Z}_d = P_{11} + P_{12}\delta_{Z_d}\left[I - P_{22}\delta_{Z_d}\right]^{-1}P_{21} \quad (50)$$

By identification, we obtain:

$$P_{Z_a} = \begin{bmatrix} Z_d & Z_d\omega_{Z_d} \\ 1 & 0 \end{bmatrix} \quad (51)$$

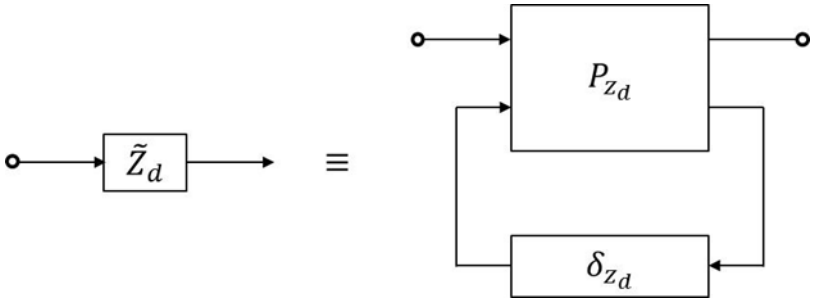

Figure 8: Simulation of $\tilde{Z}_d$

Simulation of $\frac{1}{\tilde{M}_d}$

Let use denote

$$\tilde{M}_d = M_d\left(1 + \omega_{M_d}\delta_{M_d}\right) \quad (52)$$

$$\frac{1}{\tilde{M}_d} = \frac{1}{M_d\left(1 + \omega_{M_d}\delta_{M_d}\right)} \quad (53)$$

$$\frac{1}{\tilde{M}_d} = \frac{1}{M_d} + \left(-\omega_{M_d}\right)\delta_{M_d}\left[1 - \left(-\omega_{M_d}\right)\delta_{M_d}\right]^{-1}\frac{1}{M_d} \quad (54)$$

$$\frac{1}{\tilde{M}_d} = F_l\left[P_{M_d}, \delta_{M_d}\right] \quad (55)$$

$$\frac{1}{\tilde{M}_d} = Q_{22} + Q_{21}\delta_{M_d}\left[1 - Q_{11}\delta_{M_d}\right]^{-1}Q_{12} \quad (56)$$

By identification, we obtain:

$$Q_{M_d} = \begin{bmatrix} -\omega_{M_d} & \frac{1}{M_d} \\ -\omega_{M_d} & \frac{1}{M_d} \end{bmatrix} \quad (57)$$

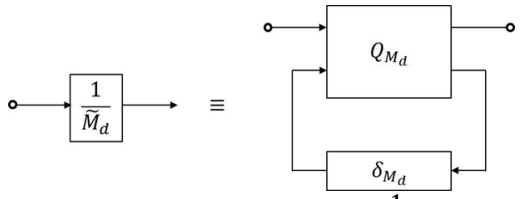

Figure 9: Simulation of $\frac{1}{\tilde{M}_d}$

Simulation of $\tilde{M}_a\tilde{Z}_d - \tilde{M}_d\tilde{Z}_a$

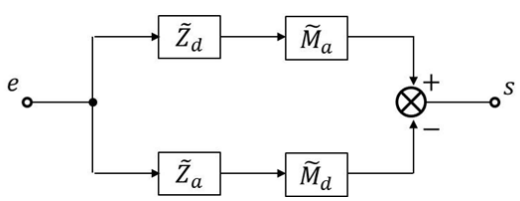

Figure 10: Simulation of $\tilde{M}_a\tilde{Z}_d - \tilde{M}_d\tilde{Z}_a$

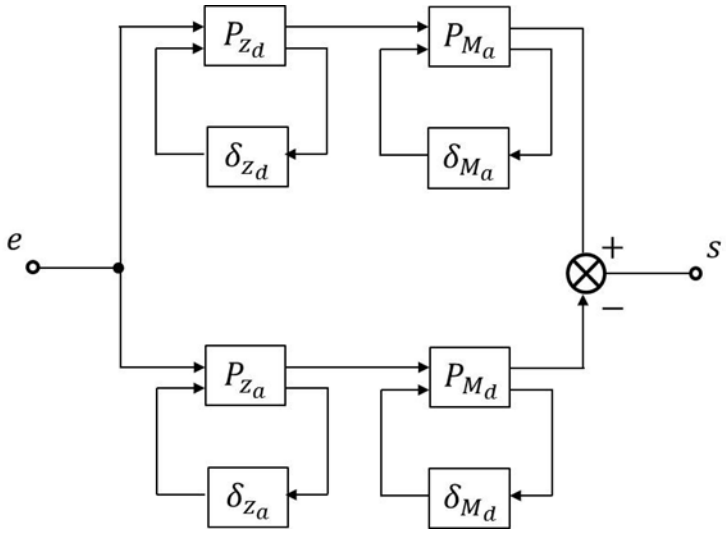

Figure 11: Simulation of $\widetilde{\boldsymbol{M}}_{\boldsymbol{a}}\widetilde{\boldsymbol{Z}}_{\boldsymbol{d}} - \widetilde{\boldsymbol{M}}_{\boldsymbol{d}}\widetilde{\boldsymbol{Z}}_{\boldsymbol{a}}$

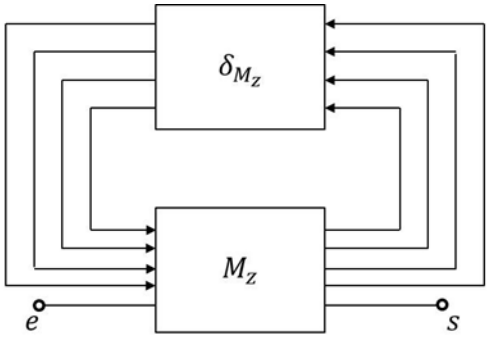

Figure 12: Simulation of $\widetilde{\boldsymbol{M}}_{\boldsymbol{a}}\widetilde{\boldsymbol{Z}}_{\boldsymbol{d}} - \widetilde{\boldsymbol{M}}_{\boldsymbol{d}}\widetilde{\boldsymbol{Z}}_{\boldsymbol{a}}$

Simulation of $\widetilde{\boldsymbol{G}}_{\boldsymbol{I}}(\boldsymbol{p})$

$$\tilde{G}_I(p) = \frac{q(p)}{\delta_c(p)} \tag{58}$$

$$\tilde{G}_I(p) = \frac{\omega_n^2\left[\widetilde{M}_d p - \widetilde{M}_d\tilde{Z}_a + \tilde{Z}_d\widetilde{M}_a\right]}{(p^2 + 2\xi\omega_n p + \omega_n^2)\left(p^2 - \tilde{Z}_a p - \widetilde{M}_a\right)} \tag{59}$$

$$\tilde{G}_I(p) = \left[\frac{\omega_n^2}{p^2 + 2\xi\omega_n p + \omega_n^2}\right]\left[\frac{\widetilde{M}_d p}{p^2 - \tilde{Z}_a p - \widetilde{M}_a} + \frac{\tilde{Z}_d\widetilde{M}_a - \widetilde{M}_d\tilde{Z}_a}{p^2 - \tilde{Z}_a p - \widetilde{M}_a}\right] \tag{60}$$

$$\tilde{G}_I(p) = G_S(p)\left[\tilde{G}_1(p) + \tilde{G}_2(p)\right] \tag{61}$$

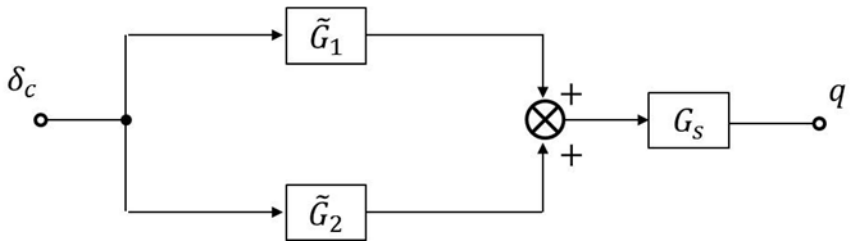

Figure 13: Simulation of $\widetilde{\boldsymbol{G}}_{\boldsymbol{I}}(\boldsymbol{p})$

$$\tilde{G}_1(p) = \frac{\widetilde{M}_d p}{p^2 - \tilde{Z}_a p - \widetilde{M}_a} \tag{62}$$

$$\tilde{G}_1(p) = \frac{V_1(p)}{E_1(p)} \tag{63}$$

$$\frac{V_1(p)}{E_1(p)} = \frac{\widetilde{M}_d p}{p^2 - \tilde{Z}_a p - \widetilde{M}_a} \tag{64}$$

$$p^2V_1(p) - \tilde{Z}_a pV_1(p) - \widetilde{M}_a V_1(p) = \widetilde{M}_d pE_1(p) \tag{65}$$

$$\ddot{v}_1(t) - \tilde{Z}_a\dot{v}_1(t) - \widetilde{M}_a v_1(t) = \widetilde{M}_d\dot{e}_1(t) \tag{66}$$

$$\ddot{v}_1(t) = \tilde{M}_d \dot{e}_1(t) + \tilde{Z}_a \dot{v}_1(t) + \tilde{M}_a v_1(t) \tag{67}$$

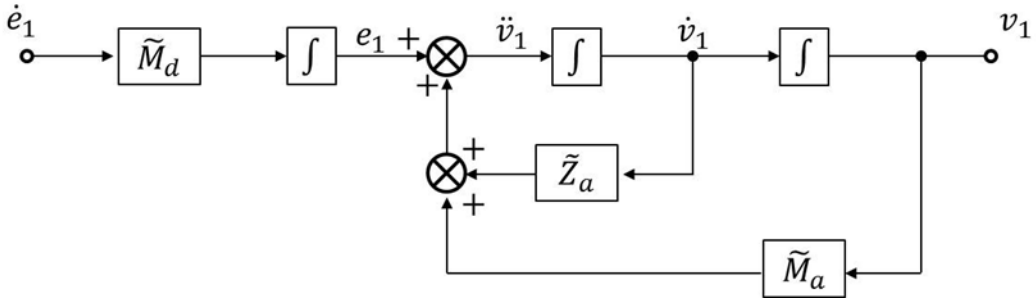

Figure 14: Simulation of $\tilde{G}_1(p)$

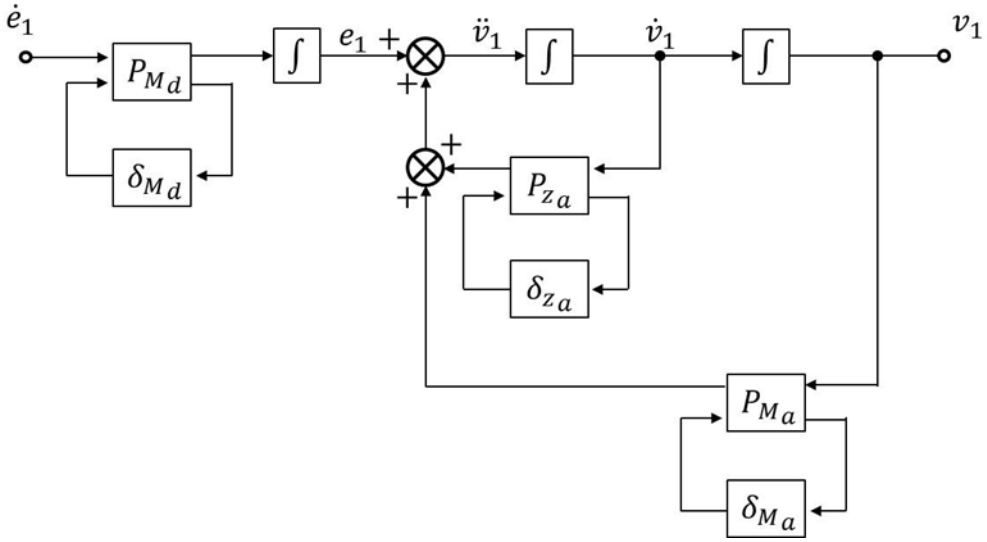

Figure 15: Simulation of $\tilde{G}_1(p)$

$$\tilde{G}_1(p) = F_u[G_1, \Delta_1] \tag{68}$$

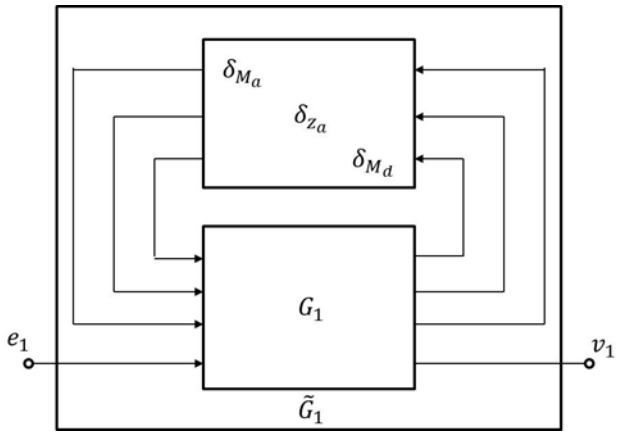

Figure 16: Simulation of $\tilde{G}_1(p)$

$$\tilde{G}_2(p) = \frac{\tilde{Z}_d \tilde{M}_a - \tilde{M}_d \tilde{Z}_a}{p^2 - \tilde{Z}_a p - \tilde{M}_a} \tag{69}$$

$$\tilde{G}_2(p) = \frac{V_2(p)}{E_2(p)} \tag{70}$$

$$\frac{V_2(p)}{E_2(p)} = \frac{\tilde{Z}_d \tilde{M}_a - \tilde{M}_d \tilde{Z}_a}{p^2 - \tilde{Z}_a p - \tilde{M}_a} \tag{71}$$

$$p^2 V_2(p) - \tilde{Z}_a p V_2(p) - \tilde{M}_a V_2(p) = \left(\tilde{Z}_d \tilde{M}_a - \tilde{M}_d \tilde{Z}_a\right) E_2(p) \tag{72}$$

$$\ddot{v}_2(t) - \tilde{Z}_a\dot{v}_2(t) - \tilde{M}_a v_2(t) = \left(\tilde{Z}_d\tilde{M}_a - \tilde{M}_d\tilde{Z}_a\right)e_2(t) \quad (73)$$

$$\ddot{v}_2(t) = \left(\tilde{Z}_d\tilde{M}_a - \tilde{M}_d\tilde{Z}_a\right)e_2(t) + \tilde{Z}_a\dot{v}_2(t) + \tilde{M}_a v_2(t) \quad (74)$$

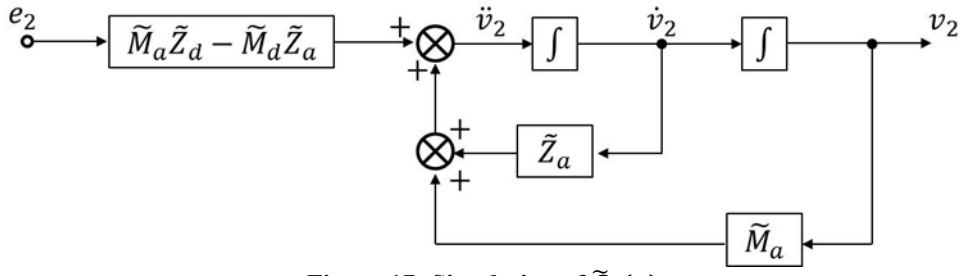

Figure 17: Simulation of $\tilde{G}_2(p)$

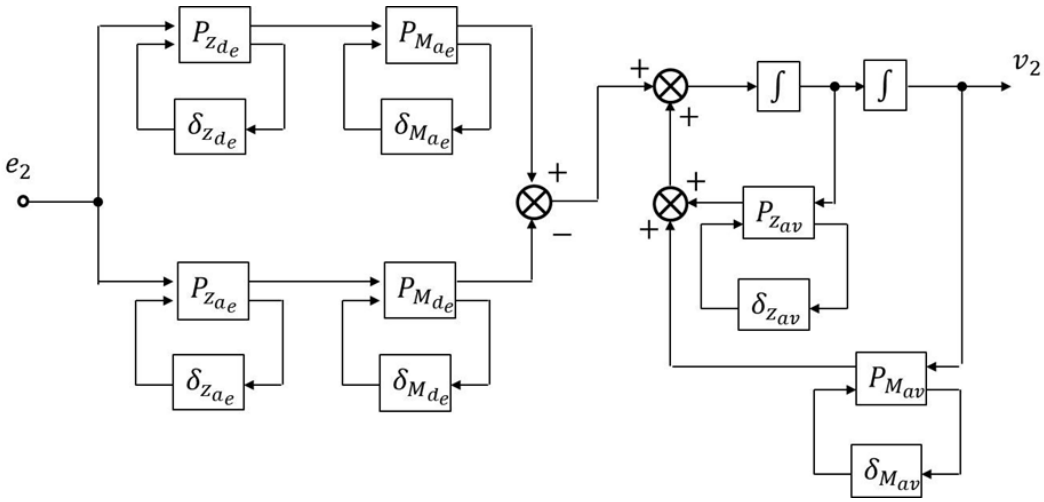

Figure 18: Simulation of $\tilde{G}_2(p)$

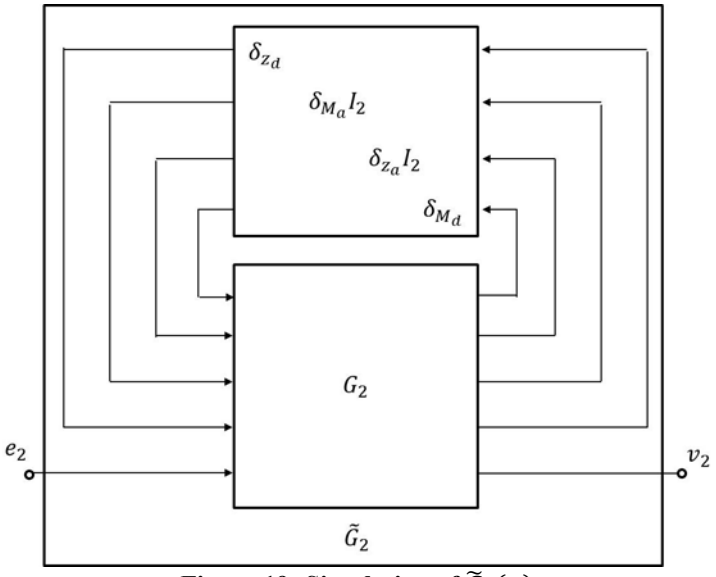

Figure 19: Simulation of $\tilde{G}_2(p)$

$$\tilde{G}_2(p) = F_u[G_2, \Delta_2] \quad (75)$$

Simulation of $G_s(p)$

$$G_s(p) = \frac{\omega_n^2}{p^2 + 2\xi\omega_n p + \omega_n^2} \quad (76)$$

$$G_s(p) = \frac{V_s(p)}{E_s(p)} \quad (77)$$

$$\frac{V_s(p)}{E_s(p)} = \frac{\omega_n^2}{p^2 + 2\xi\omega_n p + \omega_n^2} \tag{78}$$

$$p^2V_s(p) + 2\xi\omega_n pV_s(p) + \omega_n^2 V_s(p) = \omega_n^2 E_s(p) \tag{79}$$

$$\ddot{v}_s(t) + 2\xi\omega_n \dot{v}_s(t) + \omega_n^2 v_s(t) = \omega_n^2 e_s(t) \tag{80}$$

$$\ddot{v}_s(t) = \omega_n^2 e_s(t) - 2\xi\omega_n \dot{v}_s(t) - \omega_n^2 v_s(t) \tag{81}$$

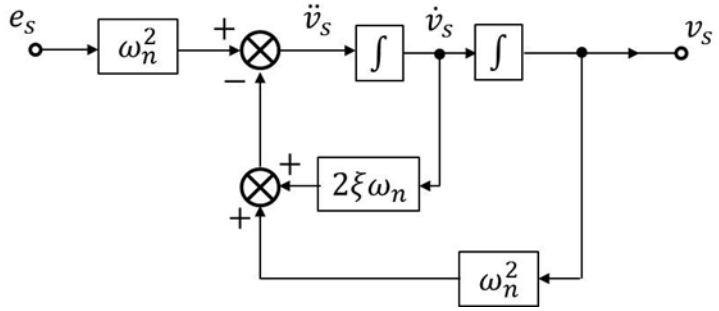

Figure 20: Simulation of $G_s(p)$

Simulation of $\tilde{G}_{II}(p)$

$$\tilde{G}_{II}(p) = \frac{A_z(p)}{q(p)} \tag{82}$$

$$\tilde{G}_{II}(p) = \frac{V\tilde{Z}_d p^2 - V\left(\tilde{Z}_d\tilde{M}_a - \tilde{Z}_a\tilde{M}_d\right)}{\tilde{M}_d p + \left(\tilde{Z}_d\tilde{M}_a - \tilde{Z}_a\tilde{M}_d\right)} \tag{83}$$

$$\tilde{G}_{II}(p) = \frac{V\tilde{Z}_d p^2}{\tilde{M}_d p + \left(\tilde{Z}_d\tilde{M}_a - \tilde{Z}_a\tilde{M}_d\right)} - \frac{V\left(\tilde{Z}_d\tilde{M}_a - \tilde{Z}_a\tilde{M}_d\right)}{\tilde{M}_d p + \left(\tilde{Z}_d\tilde{M}_a - \tilde{Z}_a\tilde{M}_d\right)} \tag{84}$$

$$\tilde{G}_{II}(p) = \tilde{G}_3(p) - \tilde{G}_4(p) \tag{85}$$

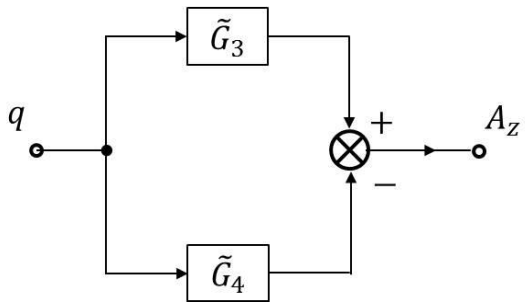

Figure 21: Simulation of $\tilde{G}_{II}(p)$

Simulation of $\tilde{G}_3(p)$

$$\tilde{G}_3(p) = \frac{V\tilde{Z}_d p^2}{\tilde{M}_d p + \left(\tilde{Z}_d\tilde{M}_a - \tilde{Z}_a\tilde{M}_d\right)} \tag{86}$$

$$\tilde{G}_3(p) = \frac{V_3(p)}{E_3(p)} \tag{87}$$

$$\frac{V_3(p)}{E_3(p)} = \frac{V\tilde{Z}_d p^2}{\tilde{M}_d p + \left(\tilde{Z}_d\tilde{M}_a - \tilde{Z}_a\tilde{M}_d\right)} \tag{88}$$

$$V_3(p)\left[\tilde{M}_d p + \left(\tilde{Z}_d\tilde{M}_a - \tilde{Z}_a\tilde{M}_d\right)\right] = V\tilde{Z}_d p^2 E_3(p) \tag{89}$$

$$V_3(p)\tilde{M}_d p + \left(\tilde{Z}_d\tilde{M}_a - \tilde{Z}_a\tilde{M}_d\right)V_3(p) = V\tilde{Z}_d p^2 E_3(p) \tag{90}$$

$$\tilde{M}_d\dot{v}_3(t) + \left(\tilde{Z}_d\tilde{M}_a - \tilde{Z}_a\tilde{M}_d\right)v_3(t) = V\tilde{Z}_d\ddot{e}_3(t) \tag{91}$$

$$\tilde{M}_d\dot{v}_3(t) = V\tilde{Z}_d\ddot{e}_3(t) - \left(\tilde{Z}_d\tilde{M}_a - \tilde{Z}_a\tilde{M}_d\right)v_3(t) \tag{92}$$

Figure 22 illustrates the simulation of $\tilde{G}_3(p)$.

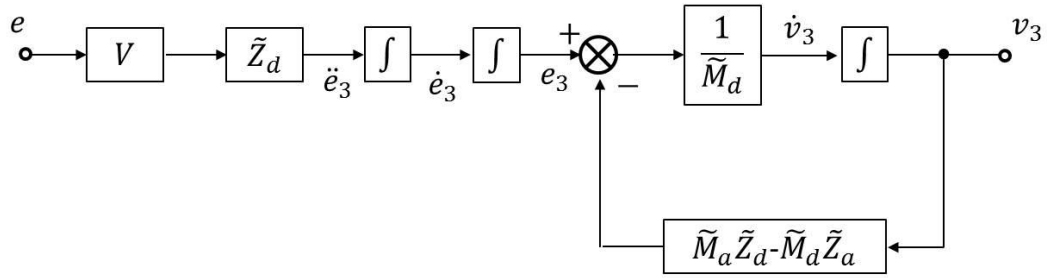

Figure 22: Simulation of $\tilde{G}_3(p)$

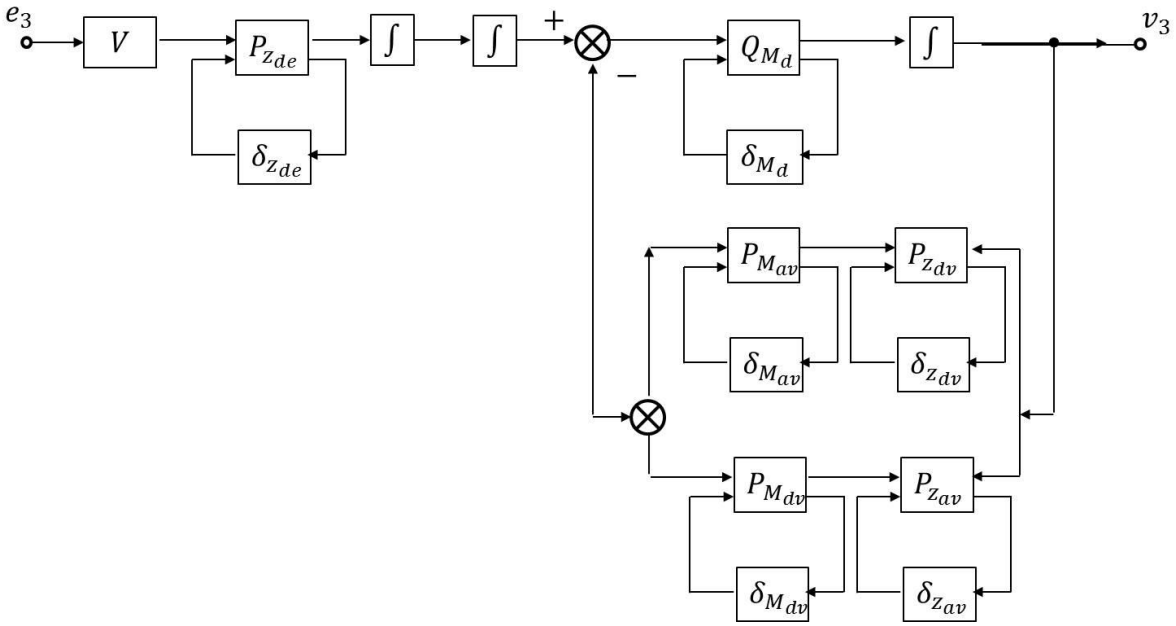

Figure 23: Simulation of $G_3(p)$

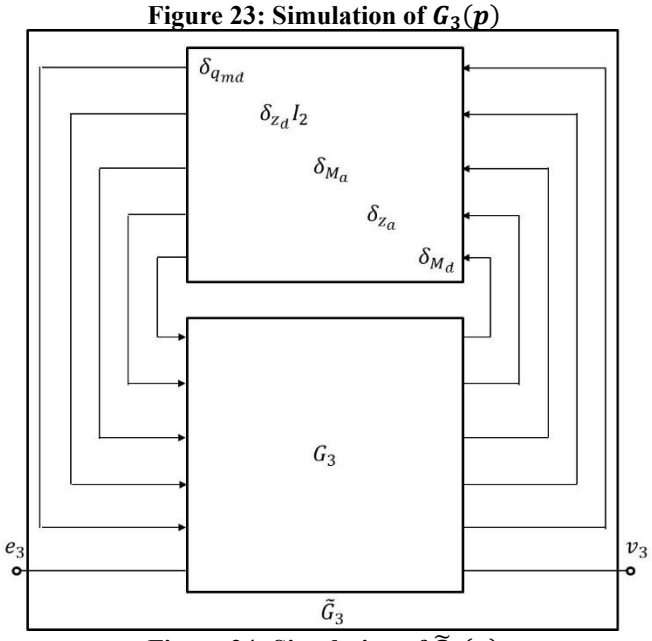

Figure 24: Simulation of $\tilde{G}_3(p)$

Simulation of $\tilde{G}_4(p)$

$$\tilde{G}_4(p) = \frac{V\left(\tilde{Z}_d\tilde{M}_a - \tilde{Z}_a\tilde{M}_d\right)}{\tilde{M}_d p + \left(\tilde{Z}_d\tilde{M}_a - \tilde{Z}_a\tilde{M}_d\right)} \tag{93}$$

$$\tilde{G}_4(p) = \frac{V_4(p)}{E_4(p)}$$

$$\frac{V_4(p)}{E_4(p)} = \frac{V\left(\tilde{Z}_d\tilde{M}_a - \tilde{Z}_a\tilde{M}_d\right)}{\tilde{M}_d p + \left(\tilde{Z}_d\tilde{M}_a - \tilde{Z}_a\tilde{M}_d\right)} \quad (94)$$

$$V_4(p)\left[\tilde{M}_d p + \left(\tilde{Z}_d\tilde{M}_a - \tilde{Z}_a\tilde{M}_d\right)\right] = V\left(\tilde{Z}_d\tilde{M}_a - \tilde{Z}_a\tilde{M}_d\right)E_4(p) \quad (95)$$

$$\tilde{M}_d p V_4(p) + \left(\tilde{Z}_d\tilde{M}_a - \tilde{Z}_a\tilde{M}_d\right)V_4(p) = V\left(\tilde{Z}_d\tilde{M}_a - \tilde{Z}_a\tilde{M}_d\right)E_4(p) \quad (96)$$

$$\tilde{M}_d \dot{v}_4(t) + \left(\tilde{Z}_d\tilde{M}_a - \tilde{Z}_a\tilde{M}_d\right)v_4(t) = V\left(\tilde{Z}_d\tilde{M}_a - \tilde{Z}_a\tilde{M}_d\right)e_4(t) \quad (97)$$

$$\tilde{M}_d \dot{v}_4(t) = V\left(\tilde{Z}_d\tilde{M}_a - \tilde{Z}_a\tilde{M}_d\right)e_4(t) - \left(\tilde{Z}_d\tilde{M}_a - \tilde{Z}_a\tilde{M}_d\right)v_4(t) \quad (98)$$

Figure 25 illustrate the simulation of $\tilde{G}_4(p)$.

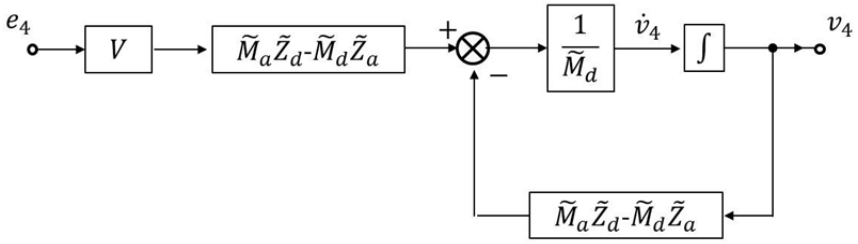

Figure 25: Simulation of $\tilde{\mathbf{G}}_4(\mathbf{p})$

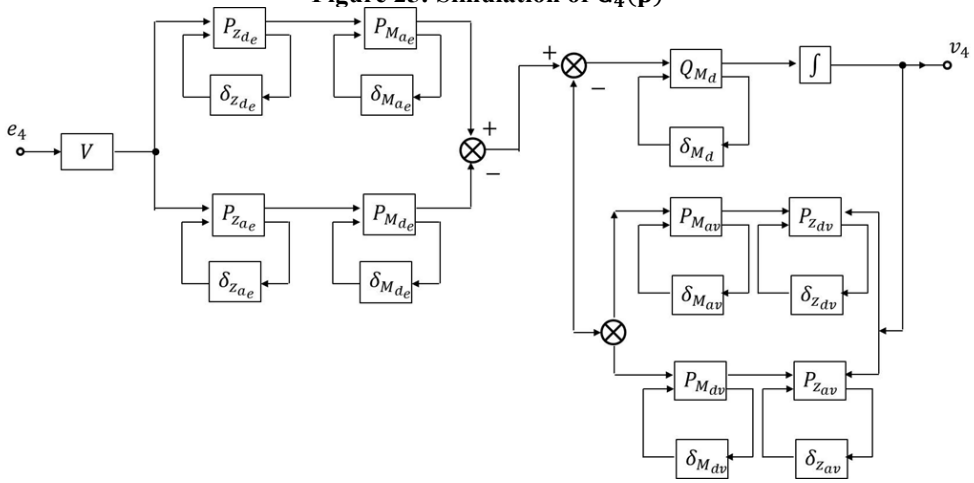

Figure 26: Simulation of $\tilde{\mathbf{G}}_4(\mathbf{p})$

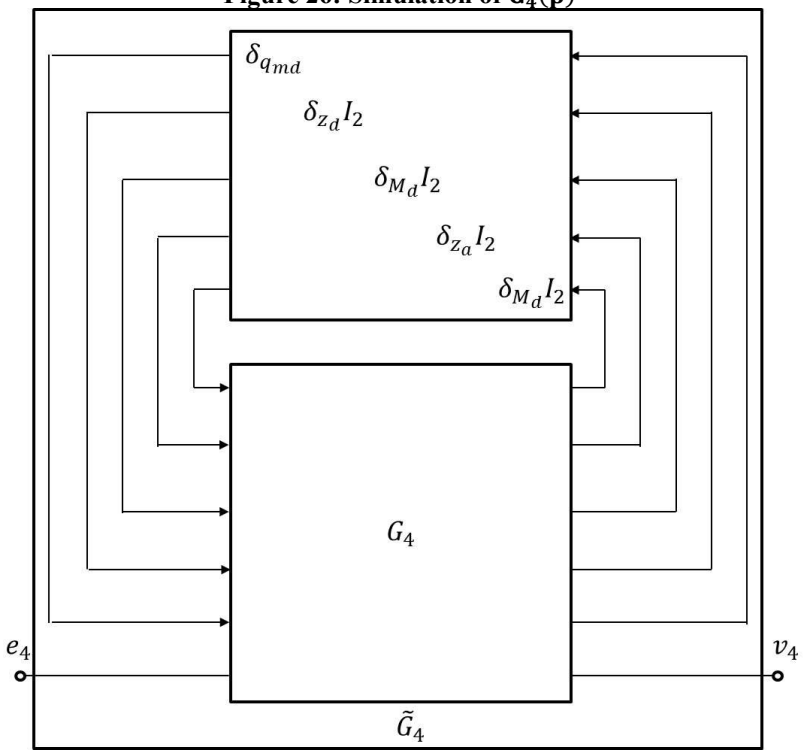

Figure 27: Simulation of $\tilde{\mathbf{G}}_4(\mathbf{p})$

Simulation of the controller $\boldsymbol{K(p)}$

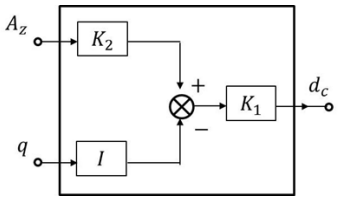

Figure 28: Simulation of the controller $\boldsymbol{K(p)}$

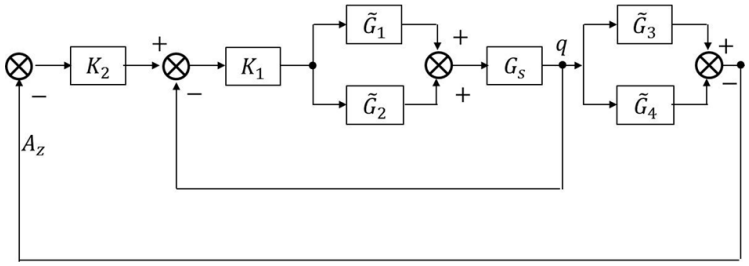

Figure 29: Simulation of the flight control system for the stability robustness study

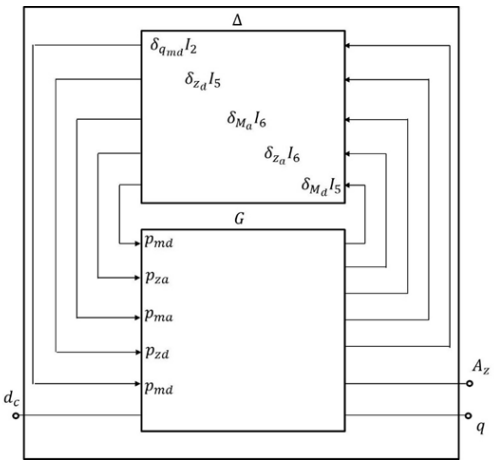

Figure 30: Simulation of $\boldsymbol{\tilde{G}(p)}$

We have :

$$\tilde{G}(p) = F_u[G, \Delta] \tag{99}$$

For the controller synthesis of this system, a direct additive model error is assumed (**Figure 31**).
The weighting selections are selected in such a way that :

$$W_1 = 10^{-1}\frac{s}{s+1}; \quad W_2 = 10^{2}\frac{1}{s+1} \tag{100}$$

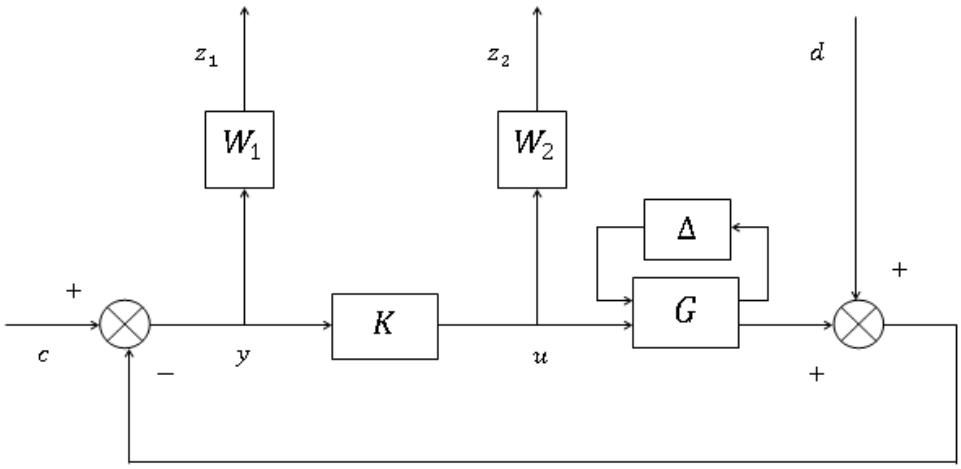

Figure 31: Block diagram of the synthesis

Mu-analysis of a missile

The block diagram for analyzing the system with structured and unstructured uncertainties in the **Figure 32**.

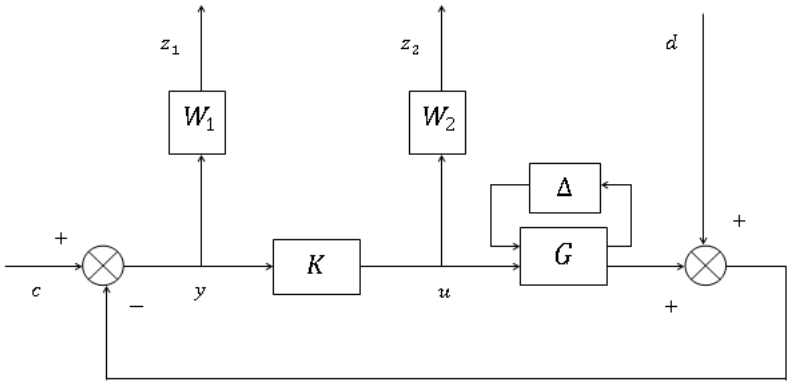

Figure 32: Block diagram of the system with structured and unstructured uncertainties

III. Result

Frequency response of the lower and upper bounds of the structured singular value of the matrix M_{22}, matrix for nominal performance analysis, of each type of controller is illustratedd in the **Figure 33**. The red curve represents the loop closure K_H and the green curve that of K_{LP}.

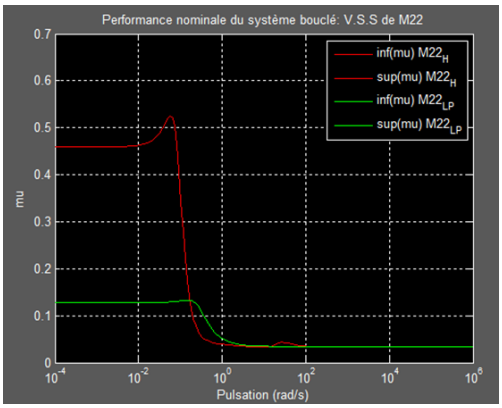

Figure 33: Analysis of the nominal performance

Table no1: Analysis of the nominal performance

Loop closure	ω_m(rad/s)	max$[\mu(M_{22})]$
K_H	0,523	0,054

The system is considered robust in performance because $\max[\mu(M_{22})] < 1$ for the two loop closures (**Table no1**).

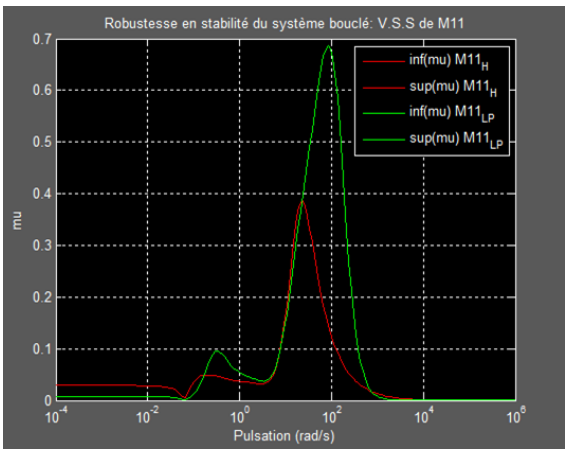

Figure 34: Analysis of the robustness in stability.

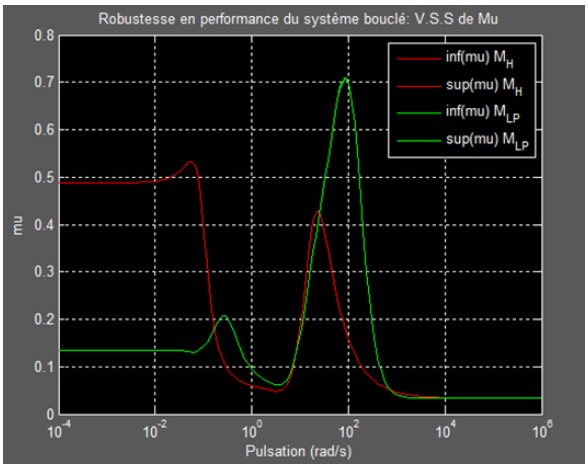

Figure 35: Analysis of the robustness in performance.

Table no 2: Analysis of the robustness in performance.

Loop closure	ω_m(rad/s)	max[$\mu(M)$]	Guarantee of the performance
K_H	0, 054	0,5369	$\|\Delta\|_\infty < \frac{1}{0,5369}$

Frequency response of the lower and upper bounds of the structured singular value of the matrix M_{11}, robustness analysis matrix for system stability, for each type of controller is shown in the **Figure 34**. The red curve corresponds to the loop closure in K_H and the green curve that of K_{LP}. Frequency response of the lower and upper bounds of the structured singular value of the matrix M_{22}, robustness analysis matrix for system performance, for each type of controller is shown in the **Figure 35**. The red curve corresponds to the loop closure in K_H and the green curve that of K_{LP}.

IV. Discussion

The system is considered stable and robust in performance for the two loop closure. A large guarantee of stability and performance for the loopback with the corrector obtained by the synthesis H_∞ is stated.

V. Conclusion

In this article, we have been able to develop robustness synthesis analysis tools for a linear system of missile. Structured singular value is one of the very powerful tools for analyzing the robustness of a linear system tainted by uncertainty. We have explained how the mu-analysis method can analyze the robustness of stability and performance of a system.

References

[1]. J. H. Blakelock, « Automatic Control Of Aircraft And Missiles », 2nd Edition, Wiley And Sons, 1991
[2]. J. N. Nielsen, « Missile Aerodynamics », 2nd Edition, Mcgraw-Hill Book Company, United States Of America, 1960.
[3]. G. M. Siouris, « Missile Guidance And Control Systems », Springer-Verlag, New York, 2004.
[4]. N. A. Shneydor, « Missile Guidance And Pursuit Kinematics, Dynamics And Control», 1st Edition, Horwood Publishing, England, 1998.
[5]. Y. Rafael, « Modern Missile Guidance », Crc Press, United States Of America, 2008.
[6]. P. Zarchan, « Tactical And Strategic Missile Guidance », 6th Edition, American Institute In Aeronautics And Astronautics, Atlanta, 2012.
[7]. B. Özkan, « Dynamic Modeling, Guidance And Control Of Homing Missiles », Natural And Applied Sciences Of Middle East Technical University, Thesis, Ankara Türkiye, September 2005.
[8]. C.W. Besserer, « Missile Engineering Handbook », D. Van Nostrand Company, New York,1958.
[9]. Y. Shtessel, C. Tournes, « Integrated Higher-Order Sliding Mode Guidance And Autopilot For Dual-Control Missiles », Aiaa Journal Of Guidance, Control And Dynamics, Vol. 32, No. 1, Pp. 79-94, 2009.
[10]. R. T. Reichert, « Dynamic Scheduling Of Modern-Robust-Control Autopilot Designs For Missiles », Ieee Control Systems Magazine, Vol. 12, No. 5, Pp. 35-42, October 1992.
[11]. W. Buzantowicz, « A Sliding Mode Controller Design For A Missile Autopilot System », Journal Of Theorical And Applied Mechanics (Poland), Vol. 58, No. 1, Pp. 169-182, 2021.
[12]. A. Mahmood, Y. Kim And J. Park, « Robust H∞ Autopilot Design Design For Agile Missile With Time-Varying Parameters », Ieee Transactions On Aerospace And Electronics Systems, Vol. 50, No. 4, Pp. 3082-3089, 10 2014.
[13]. Lee, S. Y, Lee, J-I., Ha, I-J, « Nonlinear Autopilot For High Maneuverability Of Bank-To-Turn Missiles », Ieee Transactions On Aerospace And Electronics Systems, Vol. 126, No. 1, Pp. 1236-1253, 2001.